Mathematical Biosciences 274 (2016) 12–16

Contents lists available at ScienceDirect

Mathematical Biosciences

journal homepage: www.elsevier.com/locate/mbs

Pattern formations and optimal packing

Vladimir Mityushev*

Department of Computer Sciences and Computer Methods, Pedagogical University, Podchorazych 2, Krakow 30-084, Poland

ARTICLE INFO

Article history:
Received 9 September 2015
Revised 24 January 2016
Accepted 28 January 2016
Available online 4 February 2016

Keywords:
Pattern formation
Structural approximation
Optimal packing
Random packing

ABSTRACT

Patterns of different symmetries may arise after solution to reaction–diffusion equations. Hexagonal arrays, layers and their perturbations are observed in different models after numerical solution to the corresponding initial-boundary value problems. We demonstrate an intimate connection between pattern formations and optimal random packing on the plane. The main study is based on the following two points. First, the diffusive flux in reaction–diffusion systems is approximated by piecewise linear functions in the framework of structural approximations. This leads to a discrete network approximation of the considered continuous problem. Second, the discrete energy minimization yields optimal random packing of the domains (disks) in the representative cell. Therefore, the general problem of pattern formations based on the reaction–diffusion equations is reduced to the geometric problem of random packing. It is demonstrated that all random packings can be divided onto classes associated with classes of isomorphic graphs obtained from the Delaunay triangulation. The unique optimal solution is constructed in each class of the random packings. If the number of disks per representative cell is finite, the number of classes of isomorphic graphs, hence, the number of optimal packings is also finite.

1. Introduction

The Turing mechanism for reaction–diffusion equations models biological and chemical pattern formations. This approach was widely discussed in literature and supported by many numerical examples (see the recent books [2,4,5] and many works cited therein). Patterns of different symmetries may arise after solution to reaction–diffusion equations. Hexagonal arrays, layers and their perturbations are observed in different models after numerical solution to the corresponding initial-boundary value problems for nonlinear partial differential equations. However, these models do not answer the question, why the most frequently observed patterns are close to the optimal packing structures. Why do the hexagonal array arise? One can see, for instance, that a resulting structure can be the hexagonal array disturbed by pentagon inclusions. Is it related to a model approximation or to an inherent feature of pattern formations?

In the present paper, we try to answer the above questions to demonstrate an intimate connection between pattern formations and optimal random packing on the plane. The main study is based on the following two points. First, the diffusive flux in reaction–diffusion systems is approximated by piecewise linear functions in the framework of structural approximations [3,7]. This leads to a discrete network approximation of the considered continuous problem. Second, the discrete energy minimization yields optimal random packing of the domains in the representative cell. The packed domains are approximated by equal disks. This approach is described in the bulk of the paper.

Packing problems refer to geometrical optimization problems [11]. In the present paper, we consider the optimal packing of disks on the plane in the random statement fitted to the description of pattern formations. Optimal packing in the classic deterministic statement is attained for the hexagonal array when the packing concentration holds $\frac{\pi}{\sqrt{12}}$ [11]. Computer simulations demonstrate that random packing have a lower density and depends on the protocol of the random packing [1].

It is shown in Section 3 that pattern formations lead to the optimal random packing problem in the equivalence classes of graphs obtained by means of the Delaunay triangulation. The justification of such an approach is based on the observation that solution to the physical problem of the optimal diffusion implies solution to the geometrical problem of the packing disks [8]. The unique optimal solution is constructed in each class of the random packings. If the number of disks per representative cell is finite, the number of classes of isomorphic graphs, hence, the number of optimal packings is also finite.

The proposed method to study pattern formations is based on the minimization of the discrete energy for graph structures by analytical and numerical methods within treatment of PDE by

* Corresponding author. Tel.: +48126627864; fax: +48126358858.
E-mail address: mityu@up.krakow.pl

http://dx.doi.org/10.1016/j.mbs.2016.01.008
0025-5564/

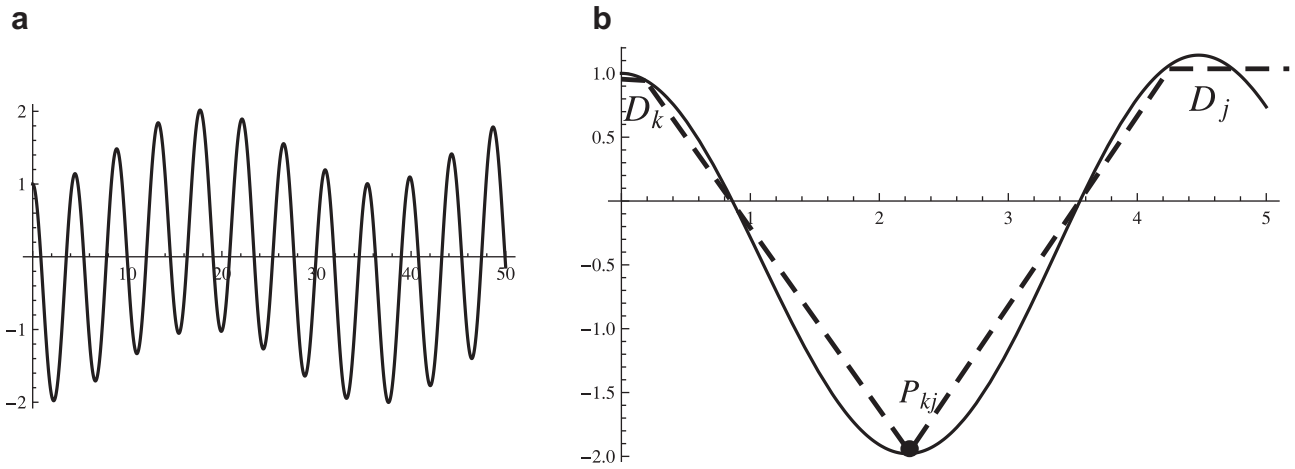

Fig. 1. (a) Dependence of the inhibitor on the spatial variable. (b) Piecewise linear approximation of the inhibitor on a smaller interval (dashed line). The maxima are approximated by segments D_k and D_j (disks in 2D) and the minima by points P_{kj} (segments in 2D).

the structural approximation method. Though PDE are not directly written in the paper, they are implicitly used in estimations of the local flux between local spatial extrema of the inhibitor.

2. Structural approximation

The Turing mechanism can create temporally stable and spatially non-homogeneous structures. In order to present the main idea of the structural approximation we consider 1D Schnakenberg system [5, p. 156]. A typical dependence of the inhibitor on the spatial variable is displayed in Fig. 1a. It is assumed that such a dependence can be approximated by a piecewise linear function as shown in Fig. 1b. The solution of the continuous reaction–diffusion equations is approximated by the discrete diffusion model with the constant diffusion fluxes (derivatives of the linear approximations) between the extrema of the potential.

A similar approximation can be extended to multidimensional reaction–diffusion equations [9]. In the present paper, we deal with 2D double periodic structures. Let $\mathbf{e}_1 = (e_1, 0)$ and $\mathbf{e}_2 = (e_{21}, e_{22})$ be the translation vectors of the lattice $\mathcal{Q} = \{l_1\mathbf{e}_1 + l_2\mathbf{e}_2 : \ l_{1,2} \in \mathbb{Z}\}$ where $\mathbb{Z}$ denotes the set of integer numbers. Consider the periodic representative cell

$$Q_0 = \{\mathbf{x} = t_1\mathbf{e}_1 + t_2\mathbf{e}_2\}, \ 0 < t_{1,2} < 1\}.$$

For simplicity, we approximate the places of maximal diffusion potential by equal disks D_i $(i = 1, 2, \dots, N)$ of radius r centered at the set of points $\mathbf{A} = (\mathbf{a}_1, \mathbf{a}_2, \dots, \mathbf{a}_N)$ displayed in Fig. 2. The maxima of the diffusion potential are approximated by disks and the minima by lines. Every line segment P_{kj} is perpendicular to the segment $(\mathbf{a}_k, \mathbf{a}_j)$, its length holds $|P_{kj}| = 2r$ and it is divided onto equal parts by $(\mathbf{a}_k, \mathbf{a}_j)$. The described approximations fits for functions of type shown in Fig. 1. Appendix contains a formal general description of the approximations.

It is convenient to introduce new distance (metric) as follows. Two points $\mathbf{a}, \mathbf{b} \in \mathbb{R}^2$ are identified if their difference $\mathbf{a} - \mathbf{b} = l_1\mathbf{e}_1 + l_2\mathbf{e}_2$ belongs to the lattice $\mathcal{Q}$. Hence, the classic flat torus topology with the opposite sides welded is introduced on the cell Q_0. The distance $\|\mathbf{a} - \mathbf{b}\|$ between two points $\mathbf{a}, \mathbf{b} \in Q_0$ is introduced as

$$\|\mathbf{a} - \mathbf{b}\| := \min_{l_1, l_2 \in \mathbb{Z}} |\mathbf{a} - \mathbf{b} + l_1\mathbf{e}_1 + l_2\mathbf{e}_2|, \tag{2.1}$$

where the modulus means the Euclidean distance in $\mathbb{R}^2$ between the points $\mathbf{a}$ and $\mathbf{b}$.

Construct the double periodic Voronoi diagram and the Delaunay triangulation corresponding to the set $\mathbf{A}$ on the torus $\mathcal{Q}_0 = \cup_{l_1, l_2 \in \mathbb{Z}}(Q_0 + l_1\mathbf{e}_1 + l_2\mathbf{e}_2)$. The edges of the Delaunay triangulation E correspond to linear approximations of the diffusion flux between disks. The Delauney triangulation of the vertices $\mathbf{A}$ consists of straight lines connecting by pairs points of $\mathbf{A}$ belonging to neighbor Voronoi regions.[1] Let the neighborhood relation between two vertexes be denoted by $\mathbf{a}_j \sim \mathbf{a}_k$ or shortly $j \sim k$. We call the constructed double periodic graph $(\mathbf{A}, E)$ by the Delaunay graph.

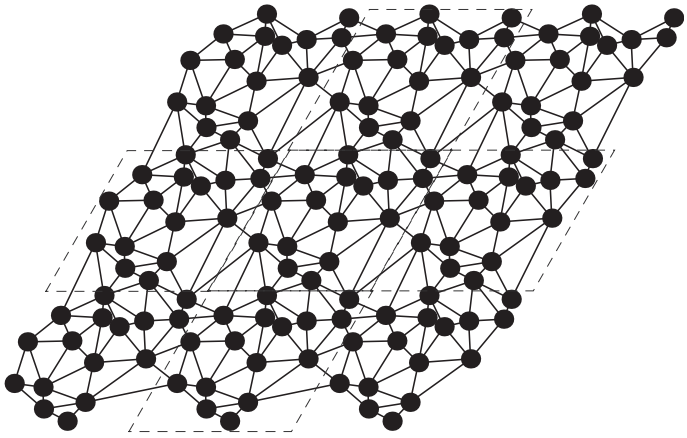

Fig. 2. 2D approximation of the inhibitor. The diffusion potential is approximated by appropriate constants in disks and the diffusion flux between the disks by linear functions along the edges of the Delaunay triangulation.

Two graphs are called isomorphic if they contain the same number of vertices connected in the same way. One of the most important notation of the present paper is the class of graphs $\mathcal{G} = \mathcal{G}_{(\mathbf{A},E)}$ isomorphic to a given graph $(\mathbf{A}, E)$.

Let $\mathbf{u} = (u_1, u_2, \dots, u_N)$ denote the vector whose components are the maximal diffusion potentials in the corresponding disks. The discrete network model for densely packed disks [3,7,10] is based on the fact that the diffusion flux is concentrated in the necks between closely spaced inclusions having different potentials. In our model, closely spaced inclusions means the chain disk–segment–disk $(D_k \leftrightsquigarrow P_{kj} \leftrightsquigarrow D_j)$ displayed in Fig. 1b. For two neighbor

[1] The terms the Delaunay triangulation and graph used in this paper are slightly different from the commonly used notations in degenerate cases. For example, consider a square and its four vertices. The traditional Delaunay triangulation has four sides of the square and one of the diagonals. In our approach, the Delaunay graph has only four sides.

disks D_k, D_j with centers $\mathbf{a}_k$, $\mathbf{a}_j$ and a segment P_{kj} between them the relative interparticle flux $g(|\mathbf{a}_k-\mathbf{a}_j|)$ can be approximated by Keller's formula [6]

$$g(\|\mathbf{a}_k-\mathbf{a}_j\|)=\pi\sqrt{\frac{r}{\delta_{kj}}}, \tag{2.2}$$

where $\delta_{kj}=\|\mathbf{a}_k-\mathbf{a}_j\|-2r$ denotes the gap between the neighbor disks. Keller's formula (2.2) was deduced for the linear local diffusion flux between the neighbor disks that is agree with our approximation. Introduce the designation

$$\sum_{k,j}^{(\mathcal{G})}=\sum_{k=1}^{N}\sum_{j\sim k}, \tag{2.3}$$

where $j\sim k$ means that the vertices $\mathbf{a}_j$ and $\mathbf{a}_k$ are connected. Following the authors in [3,7] introduce the functional associated to the discrete energy

$$E(\mathbf{u},\mathbf{a})=\sum_{k,j}^{(\mathcal{G})} g(\|\mathbf{a}_k-\mathbf{a}_j\|)(u_k+u_j)^2, \tag{2.4}$$

where u_k+u_j is the variation of the diffusion potential along the chain $D_k\rightsquigarrow P_{kj}\rightsquigarrow D_j$.

In the case of general approximations described in Appendix, the variation u_k+u_j can be replaced by u_k-u_j. The latter case corresponds to the monotonic change of the potential between two neighbor disks D_k and D_j. In particular, $u_k-u_j=0$ for touching disks. Such a change will not impact on the optimization result presented in the next section.

3. Optimal random packing

Consider the minimization problem

$$\mathcal{E}(\mathbf{u})=\min_{\mathbf{A}} E(\mathbf{u},\mathbf{A})=\min_{\mathbf{A}}\sum_{k,j}^{(\mathcal{G})} g(\|\mathbf{a}_k-\mathbf{a}_j\|)(u_k+u_j)^2. \tag{3.1}$$

The function $g(x)=\pi\sqrt{\frac{r}{x-2r}}$ as a convex function satisfies Jensen's inequality

$$\sum_{i=1}^{M} p_i g(x_i)\ge g\left(\sum_{i=1}^{M} p_i x_i\right), \tag{3.2}$$

where the sum of positive numbers p_i is equal to unity. Equality holds if and only if all x_i are equal. Let the sum from (2.4) is arranged in such a way that $x_i=\|\mathbf{a}_k-\mathbf{a}_j\|$ and $p_i=\frac{1}{U}(u_k+u_j)^2$, where $U=\sum^{(\mathcal{G})}(u_k+u_j)^2$. Application of (3.2)–(2.4) yields

$$\sum^{(\mathcal{G})} g(\|\mathbf{a}_k-\mathbf{a}_j\|)(u_k+u_j)^2\ge Ug\left(\frac{1}{U}\sum^{(\mathcal{G})}(u_k+u_j)^2\|\mathbf{a}_k-\mathbf{a}_j\|\right). \tag{3.3}$$

Hölder's inequality states that for non-negative a_i and b_i

$$\sum_{i=1}^{M} a_i b_i\le\left(\sum_{i=1}^{M} a_i^2\right)^{\frac{1}{2}}\left(\sum_{i=1}^{M} b_i^2\right)^{\frac{1}{2}}. \tag{3.4}$$

This implies that

$$\sum^{(\mathcal{G})}(u_k+u_j)^2\|\mathbf{a}_k-\mathbf{a}_j\|\le\left[\sum^{(\mathcal{G})}(u_k+u_j)^4\right]^{\frac{1}{2}}\left[\sum^{(\mathcal{G})}\|\mathbf{a}_k-\mathbf{a}_j\|^2\right]^{\frac{1}{2}}. \tag{3.5}$$

The function $g(x)$ decreases, hence (3.3) and (3.5) give

$$\frac{1}{U}\sum^{(\mathcal{G})} g(\|\mathbf{a}_k-\mathbf{a}_j\|)(u_k+u_j)^2 \ge g\left(\frac{1}{U}\left[\sum^{(\mathcal{G})}(u_k+u_j)^4\right]^{\frac{1}{2}}\left[\sum^{(\mathcal{G})}\|\mathbf{a}_k-\mathbf{a}_j\|^2\right]^{\frac{1}{2}}\right). \tag{3.6}$$

The minimum of the right hand part of (3.6) on $\mathbf{A}$ is achieved independently on u_k for $\max_{\mathbf{A}} h(\mathbf{A})$ where

$$h(\mathbf{A})=\sum^{(\mathcal{G})}\|\mathbf{a}_k-\mathbf{a}_j\|^2. \tag{3.7}$$

Lemma 3.1 ([9]). *For any fixed class $\mathcal{G}_{(\mathbf{A},E)}$, every local maximizer of $h(\mathbf{A})$ is the global maximizer which fulfils the system of linear algebraic equations*

$$\mathbf{a}_k=\frac{1}{N_k}\sum_{j\sim k}\mathbf{a}_j+\frac{1}{N_k}\sum_{\ell=1,2} s_{k\ell}\mathbf{e}_\ell,\quad k=1,2,\dots,N, \tag{3.8}$$

where $s_{k\ell}$ can take the values $0,\pm1,\pm2$ in accordance with the class $\mathcal{G}_{(\mathbf{A},E)}$. The system (3.8) has always a unique solution up to an additive arbitrary constant vector.

Equations (3.8) describe the stationary points of the functional (3.7) obtained by its differentiation on $\mathbf{a}_k$ $(k=1,2,\dots,N)$

$$\sum_{j\sim k}(\mathbf{a}_j-\mathbf{a}_k)\equiv\mathbf{0}. \tag{3.9}$$

Here, the congruence relation $\mathbf{a}\equiv\mathbf{b}$ means that $\mathbf{a}-\mathbf{b}=l_1\mathbf{e}_1+l_2\mathbf{e}_2$ for some integer $l_{1,2}$. Therefore, a point $\mathbf{a}$ on the torus $\mathcal{Q}_0$ is associated to the infinite set of points $\{\mathbf{a}+l_1\mathbf{e}_1+l_2\mathbf{e}_2,\ l_{1,2}\in\mathbb{Z}\}$ on the plane $\mathbb{R}^2$. We now rewrite equation (3.9) on the torus as an equation on the plane for a fixed point $\mathbf{a}_k\in Q_0$. Consider a points $\mathbf{a}'_j\in\mathbb{R}^2$ neighboring to $\mathbf{a}_k$, i.e., $j\sim k$ in a graph $(\mathbf{A},E)\in\mathcal{G}_{(\mathbf{A},E)}$. The point $\mathbf{a}'_j$ is congruent to a point $\mathbf{a}_j\in Q_0$. The graph $(\mathbf{A},E)$ corresponds to the Voronoi tessellation, hence, $\mathbf{a}'_j$ belongs to Q_0 or to neighbor cells $Q_0\pm\mathbf{e}_1$, $Q_0\pm\mathbf{e}_2$, $Q_0\pm\mathbf{e}_1\pm\mathbf{e}_2$. Therefore, $\mathbf{a}'_j=\mathbf{a}_j+l_{1jk}\mathbf{e}_1+l_{2jk}\mathbf{e}_2$, where l_{1jk} and l_{2jk} can be equal only to 0, ±1. Then, equations (3.9) can be written in the form (3.8) where

$$s_{1k}=\sum_{j\sim k} l_{1jk},\quad s_{2k}=\sum_{j\sim k} l_{2jk}. \tag{3.10}$$

One can see that the sum of all equations (3.8) gives an identity, hence, they are linearly dependent. Moreover, if $\mathbf{A}=(\mathbf{a}_1,\mathbf{a}_2,\dots,\mathbf{a}_N)$ is a solution of (3.8), then $(\mathbf{a}_1+\mathbf{c},\mathbf{a}_2+\mathbf{c},\dots,\mathbf{a}_N+\mathbf{c})$ is also a solution of (3.8) for any $\mathbf{c}\in\mathbb{R}^2$. Let the point $\mathbf{a}_N$ be arbitrarily fixed. Then, $\mathbf{a}_1,\mathbf{a}_2,\dots,\mathbf{a}_{N-1}$ can be found from the uniquely solvable system of linear algebraic equations

$$\mathbf{a}_k=\frac{1}{N_k}\sum_{j\sim k}\mathbf{a}_j+\frac{1}{N_k}\sum_{\ell=1,2} s_{k\ell}\mathbf{e}_\ell,\quad k=1,2,\dots,N-1. \tag{3.11}$$

It is worth noting that the system (3.11) can be decomposed onto two independent systems of scalar equations on the first and second coordinates of the points $\mathbf{a}_1,\mathbf{a}_2,\dots,\mathbf{a}_{N-1}$.

4. Numerical examples

We now proceed to summarize the algorithm to solve the optimization problem. First, let a class of graphs $\mathcal{G}_{(\mathbf{A},E)}$ be fixed with the corresponding translation vectors $\mathbf{e}_1$ and $\mathbf{e}_2$. The main step is solution to the minimization problem (3.1). In the present paper, we consider examples of the simplified optimization problem when the vertices $\mathbf{A}$ satisfy the uniquely solvable system of linear algebraic equations (3.11) with fixed $s_{k\ell}$. The corresponding double periodic Delaunay graph $(\mathbf{A},E)$ is called optimal in the class $\mathcal{G}_{(\mathbf{A},E)}$. In such a simplified statement it satisfies the optimization problem (3.1) if the inequality (3.6) become equality. The optimal graph not necessary does correspond to a Voronoi tessellation. In this case, one can change a class of graphs by introduction of the new Voronoi tessellation for the vertices $\mathbf{A}$. Then, the set $\mathbf{A}$ will not necessary be optimal in the new class $\mathcal{G}'_{\mathbf{A}}$. Let $(\mathbf{A}',E')$ be the optimal graph in the class $\mathcal{G}'_{\mathbf{A}}$. Next, if the graph $(\mathbf{A}',E')$ does not correspond to a Voronoi tessellation, it can be "improved" by $(\mathbf{A}'',E'')$, etc. Therefore, we arrive at the graph chain

$$(\mathbf{A},E)\to(\mathbf{A}',E')\to(\mathbf{A}'',E'')\to\cdots. \tag{4.1}$$

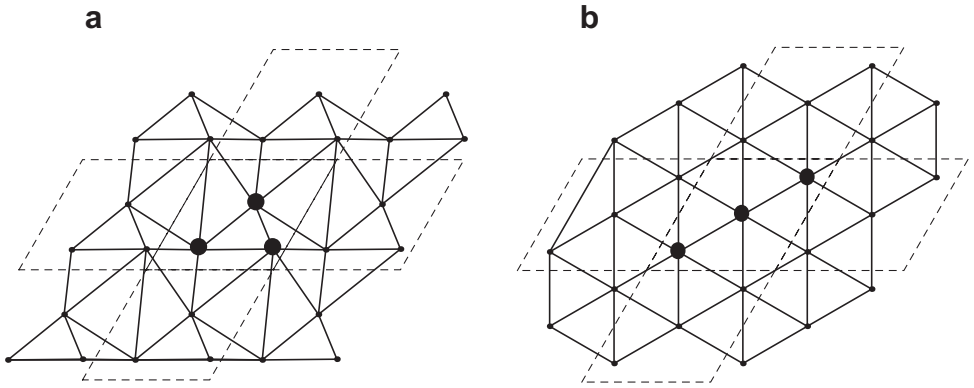

Fig. 3. (a) Three points in the cell Q_0 are distinguished. Dashed lines show the lattice, solid lines the double periodic Delaunay graph. (b) The optimal graph isomorphic to the graph from (a).

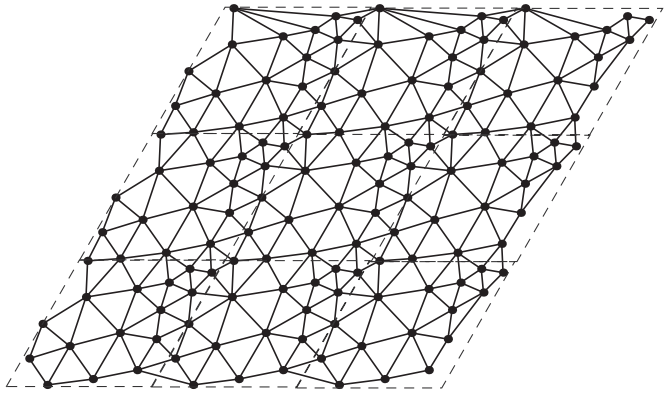

Fig. 4. The optimal graph $(\mathbf{A}', E')$ from Example 4.2.

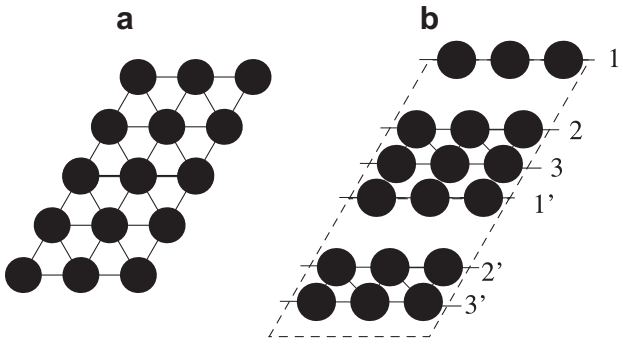

Fig. 5. The optimal graphs from Example 4.3. The disks in the layers 1 and 1', 2 and 2', 3 and 3' are the same in the toroidal topology.

Example 4.1. Consider the hexagonal lattice defined by the fundamental translation vectors $\mathbf{e}_1 = \sqrt[4]{\frac{4}{3}}(1, 0)$ and $\mathbf{e}_2 = \sqrt[4]{\frac{4}{3}}(\frac{1}{2}, \frac{\sqrt{3}}{2})$. The area of the cell Q_0 holds unit. Consider $N = 3$ points (1.075, 0.175), (0.919, 0.553), (0.444, 0.169) and the corresponding double periodic Voronoi tessellation shown in Fig. 3a.

Application of the algorithm yields the optimal hexagonal structure (Fig. 3b).

Example 4.1 is a simple illustration of the general result that the class of regular graphs for which every vertex has six neighbors contains the unique optimal graph corresponding to the regular hexagonal lattice.

Example 4.2. Consider the hexagonal lattice as in Example 4.1 and $N = 16$ points with the corresponding double periodic Voronoi tessellation shown in Fig. 2. The considered structure determines a double periodic graph $(\mathbf{A}, E)$. This graph generates the class of isomorphic graphs $\mathcal{G}_{(\mathbf{A},E)}$. Find the optimal graph $(\mathbf{A}', E)$ in the class $\mathcal{G}_{(\mathbf{A},E)}$. Construct the Voronoi tessellation corresponding to the set $\mathbf{A}'$ and the corresponding graph $(\mathbf{A}', E')$ which determines the new class $\mathcal{G}'_{(\mathbf{A}',E')}$. The optimal graph in the class $\mathcal{G}'_{(\mathbf{A}',E')}$ is the graph $(\mathbf{A}', E')$. Therefore, in this example the graph $(\mathbf{A}, E)$ from Fig. 2 is transformed into the graph $(\mathbf{A}', E')$ from Fig. 4.

Compare a regular graph where each vertex has 6 neighbors with the graph $(\mathbf{A}', E')$ from Fig. 4. This comparison demonstrates that fluctuations of the number 6 lead to other optimal structures. Thus, the optimal graph $(\mathbf{A}', E')$ from Fig. 4 contains five vertices with five neighbors, seven vertices with six neighbors, three vertices with seven neighbors and one vertex with eight neighbors.

Every edge of the Delaunay graph models the interaction caused by the diffusion flux. This flux between two disks can be insignificant if the gap between the disk is sufficiently large. The local low flux can be caused by a biological mechanism. In this case, the corresponding edge should be deleted from the Delaunay graph. We consider such a case in the following example.

Example 4.3. Consider $N = 9$ points and the double periodic Voronoi tessellation isomorphic to the hexagonal lattice. The perfect hexagonal array in Fig. 5a presents the optimal graph $(\mathbf{A}, E)$. Consider another graph $(\mathbf{A}, E')$ obtained from $(\mathbf{A}, E)$ by deletion of the edges connecting the first layer of disks with other layers. In this case, the optimal graph becomes similar to hexagonal-layered structure displayed in Fig. 5b.

The above examples illustrate few scenarios of the 2D pattern formations. Systematic simulations of the general minimization problem (3.1) can help to study properties of the optimal graphs.

5. Conclusions

The main feature of the proposed method is investigation of the graph structures by analytical and numerical methods. The method of structural approximation recalls a finite element method when a continuous problem is approximated by a discrete problem. The structural approximation is based on a "physical discretization" [3], when edges of the graph correspond to the most intensive places of the diffusion flux. Further, the principle of minimum energy yields a discrete numerical problem as in a finite element method. The method of structural approximation was justified for the p-Laplacian including linear equations in [3,7,10].

We note that the discrete energy (2.4) and the corresponding continuous energy [3,7] can be considered independently on the reaction–diffusion and other PDE. It is interesting to note that Lemma 3.1 holds for an arbitrary interparticle flux $g(\|\mathbf{a}_k-\mathbf{a}_j\|)$ satisfying the following two conditions: (i) $g(\|\mathbf{a}_k-\mathbf{a}_j\|)$ tends to infinity, as $\delta_{kj}=\|\mathbf{a}_k-\mathbf{a}_j\|-2r$ tends to zero; (ii) the function g is convex.

The structural approximation approach was applied in [3,7] for fixed geometries, i.e., for given locations of disks and their radii. The energy (2.4) was minimized on the potential values $\mathbf{u}=(u_1,u_2,\dots,u_N)$. In the present paper, we consider the energy minimization (3.1) on the geometric parameters $\mathbf{A}$ and demonstrate emergence of the optimal structures. Moreover, we introduced "hidden" optimal structures by introduction of the classes of graphs. For instance, a pentagon embedded in the hexagonal structure can also form an optimal structure. All the possible optimal structures are estimated in Lemma 3.1. This is the main result of the paper. Further analysis can be performed following the structural approximations [3,7,10] by the energy minimization (2.4) on $\mathbf{u}$ with fixed geometry. It can be done by fitting of $\mathbf{u}$ to the considered PDE.

The structural approximation method is numerically effective for systems of PDE with large numbers of equations when the traditional methods lead to numerical solution to huge system of linear and nonlinear algebraic equations. Advantages take also place for spatially high oscillating solutions of PDE (see [3,7,10] and works cited therein). Let d denote the linear size of the "smoothed" extremum (the domains D_k and D_j in Fig. 1b) and δ the distance between neighbor extrema (the distance between D_k and D_j). Analytical estimations and numerical simulations [3,7] demonstrate an excellent numerical precision of the structural approximations for $\frac{\delta}{d}<0.2$ which decreases when $\frac{\delta}{d}$ increases. The number of "smoothed" extrema per cell, N, is of order of oscillations per cell. It should be taken a priory sufficiently large to get a sufficiently precise solution. However, in pattern formation it is interesting to qualitatively determine the type of patterns. For instance, the hexagonal and layer patterns can be predicted for $N=9$ in Example 4.3. It is worth noting that all computational examples in the present paper require at most 10 s of CPU time.

We suggest that natural patterns can be reduced to the optimal structures which minimize the energy (2.4). Then, the presented theoretical study can be used in biological research to classify the patterns after advanced computer simulations and observation of the real biological structures. The diversity of patterns is determined by classes of isomorphic graphs. If the number N of vertices per representative cell is finite, then the number of classes, hence the number of optimal structures, is also finite.

For simplicity, we approximate the high potential domains by disks and points in the above figures. Actually, the disks can schematically present domains of other shapes. For instance, series of disks in Fig. 5b can be approximated by strips corresponding to the 1D optimization. Example 4.3 demonstrates that anisotropic structure of graphs can lead to the anisotropic strip structures. In particular, this means that the strip structure is optimal in the corresponding class of graphs. It is interesting to describe the biological reasons of local anisotropy modeled by edges of graphs.

In the following concluding remark, we want to stress that the method of division onto isomorphic graphs can be applied to another problem concerning simulations of random packings [1].

Remark 5.1. Solution to the optimal energy problem yields solution to the optimal packing problem for disks [8] and for spheres in $\mathbb{R}^d$ [9]. The corresponding concentration $\nu(\mathcal{G})$ of disks attains the maximal value in the class $\mathcal{G}_{(\mathbf{A},E)}$. The set of optimal graphs includes graphs corresponding to packing constructed by various packing protocols. This scheme gives the set of the optimal concentrations depending on protocols, i.e., on the class of graphs and essentially reduce computations. Because in order to get the set of all optimal packings, it is sufficient to determine the target vertices $\mathbf{A}$ of the optimization problems (3.1) in all classes of graphs.

Acknowledgment

The author thanks the anonymous reviewers for their valuable comments and suggestions to improve the paper and further to develop the obtained results.

Appendix

This section is devoted to justification that any function $f(\mathbf{x})$ continuously differentiable on a closed smooth connected domain Q can be approximated by a function of the special type called here the packing function.

First, for any positive ε the function $f(\mathbf{x})$ can be approximated by a piecewise constant function $f_\varepsilon(\mathbf{x})$ in such a way that $\|f(\mathbf{x})-f_\varepsilon(\mathbf{x})\|<\varepsilon$, $\mathbf{x}\in Q$. Let $S_{\nu j}$ denote a connected component of the domain where $f_\varepsilon(\mathbf{x})=\nu$ $(j=1,2,\dots,J_\nu)$. The set

$$\{S_{\nu j}:\nu\in[\min_{\mathbf{x}\in Q}f_\varepsilon(\mathbf{x}),\max_{\mathbf{x}\in Q}f_\varepsilon(\mathbf{x})],\ j=1,2,\dots,J_\nu\}$$

generates a finite partition of Q. Let $|S_{\nu j}|$ denote the area of $S_{\nu j}$. Each domain $S_{\nu j}$ can be filled by sufficiently small non-overlapping disks (touching is possible) in such a way that the boundary chain of touching disks with its interior forms a domain $\widetilde{S}_{\nu j}\subset S_{\nu j}$ for which $|S_{\nu j}|-|\widetilde{S}_{\nu j}|<\varepsilon$. The piecewise constant function $f_\varepsilon(\mathbf{x})$ can be approximated by a continuous function $\widetilde{f}_\varepsilon(\mathbf{x})$ equal to $f_\varepsilon(\mathbf{x})$ on all $\widetilde{S}_{\nu j}$; $\widetilde{f}_\varepsilon(\mathbf{x})$ is represented by ruled surfaces between every two neighboring $\widetilde{S}_{\nu j}$.

Thus, any continuously differentiable function $f(\mathbf{x})$ on a connected closed domain $Q\subset\mathbb{R}^2$ with smooth boundary can be approximated by a packing function $\widetilde{f}_\varepsilon(\mathbf{x})$. More precisely, $\widetilde{f}_\varepsilon(\mathbf{x})$ converges pointwise to $f(\mathbf{x})$, as $\varepsilon\to 0$. In particular, any continuously differentiable solution of the reaction–diffusion equations can be approximated by packing functions.

References

[1] S. Atkinson, F.H. Stillinger, S. Torquato, Existence of isostatic, maximally random jammed monodisperse hard-disk packings, Proc. Natl. Acad. Sci. USA 111 (2014) 18436–18441.
[2] P.C. Bressloff, Stochastic Processes in Cell Biology, Springer International Publishing Switzerland, New York, 2014.
[3] L. Berlyand, A.G. Kolpakov, A. Novikov, Introduction to the Network Approximation. Method for Materials Modeling, Cambridge University Press, Cambridge, 2013.
[4] N. Ghoniem, D. Walgraef, Instabilities and Self-Organization in Materials, Vols. 1–2, Oxford University Press, Oxford, 2008.
[5] J. Jost, Mathematical Methods in Biology and Neurobiology, Springer, London, 2014.
[6] J.B. Keller, Conductivity of a medium containing a dense array of perfectly conducting spheres or cylinders or nonconducting cylinders, J. Appl. Phys. 34 (1963) 991–993.
[7] A.A. Kolpakov, A.G. Kolpakov, Capacity and Transport in Contrast Composite Structures: Asymptotic Analysis and Applications, CRC Press, Boca Raton, 2010.
[8] V. Mityushev, N. Rylko, Optimal distribution of the non-overlapping conducting disks, Multiscale Model. Simul. 10 (2012) 180–190.
[9] V. Mityushev, Optimal packing of spheres in $\mathbb{R}^d$ and extremal effectiveconductivity, 2014, arXiv:1412.7527.
[10] N. Rylko, Structure of the scalar field around unidirectional circular cylinders, Proc. R. Soc. A464 (2008) 391–407.
[11] L.F. Tóth, Lagerungen in der Ebene auf der Kugel und im Raum, Springer-Verlag, Berlin, 1953.